Molecular Biology of the Cell
Vol. 18, 2667–2677, July 2007

Cholesterol Controls Lipid Endocytosis through Rab11[D]

Miwa Takahashi,*† Motohide Murate,* Mitsunori Fukuda,‡§ Satoshi B. Sato,*‖ Akinori Ohta,† and Toshihide Kobayashi*¶#

*Frontier Research System, ‡Fukuda Initiative Research Unit, and ¶Lipid Biology Laboratory, RIKEN, Wako, Saitama 351-0198, Japan; †Department of Biotechnology, The University of Tokyo, Bunkyo-ku, Tokyo 113-8657, Japan; §Department of Developmental Biology and Neurosciences, Graduate School of Life Sciences, Tohoku University, Miyagi 980-8578, Japan; ‖Department of Biophysics, Graduate School of Science, Kyoto University, Kyoto 606-8502, Japan; and #Institut National de la Santé et de la Recherche Médicale U870, Institut National de la Recherche Agronomique U1235, Institut National des Sciences Appliquées de Lyon, University Lyon 1 and Hospices Civils de Lyon, 69621 Villeurbanne, France

Submitted October 17, 2006; Revised April 20, 2007; Accepted April 24, 2007
Monitoring Editor: Robert Parton

Cellular cholesterol increases when cells reach confluency in Chinese hamster ovary (CHO) cells. We examined the endocytosis of several lipid probes in subconfluent and confluent CHO cells. In subconfluent cells, fluorescent lipid probes including poly(ethylene glycol)derivatized cholesterol, 22-(*N*-(7-nitrobenz-2-oxa-1,3-diazol-4-yl)amino)-23,24-bisnor-5-cholen-3β-ol, and fluorescent sphingomyelin analogs were internalized to pericentriolar recycling endosomes. This accumulation was not observed in confluent cells. Internalization of fluorescent lactosylceramide was not affected by cell confluency, suggesting that the endocytosis of specific membrane components is affected by cell confluency. The crucial role of cellular cholesterol in cell confluency–dependent endocytosis was suggested by the observation that the fluorescent sphingomyelin was transported to recycling endosomes when cellular cholesterol was depleted in confluent cells. To understand the molecular mechanism(s) of cell confluency– and cholesterol-dependent endocytosis, we examined intracellular distribution of rab small GTPases. Our results indicate that rab11 but not rab4, altered intracellular localization in a cell confluency–associated manner, and this alteration was dependent on cell cholesterol. In addition, the expression of a constitutive active mutant of rab11 changed the endocytic route of lipid probes from early to recycling endosomes. These results thus suggest that cholesterol controls endocytic routes of a subset of membrane lipids through rab11.

INTRODUCTION

Little is known about the mechanisms of internalization of plasma membrane lipids and lipid domains. Recent studies using various lipid probes revealed different endocytic pathways of plasma membrane lipids (Kok *et al.*, 1991; Mukherjee *et al.*, 1999; Puri *et al.*, 2001; Hao *et al.*, 2002; Maxfield and Wustner, 2002; Pagano, 2003; Sato *et al.*, 2004). Targeted trafficking of lipid probes might be due to the differential partitioning preference of these lipids and lipid analogs in coexisting lateral membrane domains of varying chemical composition and physical properties (Mukherjee *et al.*, 1999). Alteration of cellular cholesterol level affects the endocytosis of lipid analogs. The addition of cholesterol stimulates the uptake of fluorescent lactosylceramide (LacCer) analog (Sharma *et al.*, 2004). It is also reported that different lipid probes are differently affected by cholesterol. In normal skin fibroblasts, both fluorescent LacCer and fluorescent sphingomyelin are internalized into the Golgi apparatus. However, fluorescent LacCer, but not sphingomyelin, is transported to the late endosomes/lysosomes in Niemann-Pick fibroblasts or when cellular cholesterol is elevated in normal skin fibroblasts (Puri *et al.*, 1999, 2001). When cholesterol is depleted, long-chain 1,1′-dioctadecyl-3,3,3′,3′-tetramethylindocarbocyanine perchlorate (DiI) analogs are sorted to the recycling pathway instead of going to the late endosomes/lysosomes, whereas the endocytosis of short chain DiI analog is inhibited under these conditions (Hao *et al.*, 2004).

Rab proteins also regulate lipid transport. Overexpression of rab11 results in accumulation of cholesterol, pyrene-labeled sphingomyelin analog, and sulfatide in rab11-positive organelles (Holtta-Vuori *et al.*, 2002). Esterification of cholesterol is inhibited under these conditions. Transfection of dominant-negative form of rab7 or rab9 in normal human fibroblasts disrupts Golgi targeting of the fluorescent LacCer analog (Choudhury *et al.*, 2002). Interestingly, overexpression of wild-type rab7 and rab9 in Niemann-Pick fibroblasts results in correction of fluorescent LacCer trafficking and reductions in intracellular cholesterol stores (Choudhury *et al.*, 2002; Walter *et al.*, 2003; Narita *et al.*, 2005). Similarly, overexpression of rab8 rescues the late endosomal choles-

This article was published online ahead of print in *MBC in Press* (http://www.molbiolcell.org/cgi/doi/10.1091/mbc.E06–10–0924) on May 2, 2007.

[D] The online version of this article contains supplemental material at *MBC Online* (http://www.molbiolcell.org).

Address correspondence to: Toshihide Kobayashi (kobayasi@riken.jp).

Abbreviations used: PEG-cholesterol, poly(ethylene glycol)-derivatized cholesterol; NBD-SM, *N*-((6-(7-nitrobenz-2-oxa-1,3-diazol-4-yl)amino)hexanoyl)sphingosylphosphorylcholine; BODIPY-SM, *N*-(4,4-difluoro-5,7-dimethyl-4-bora-3a,4a-diaza-s-indacene-3-pentanoyl)sphingosylphosphorylcholine; NBD-cholesterol, 22-(*N*-(7-nitrobenz-2-oxa-1,3-diazol-4-yl)amino)-23,24-bisnor-5-cholen-3β-ol.

terol deposition and sphingolipid mistargetting in Niemann-Pick fibroblasts (Linder *et al.*, 2007). It is also reported that the microinjection of rab-guanine nucleotide dissociation inhibitor (GDI) inhibits late endosomal/lysosomal cholesterol mobilization (Holtta-Vuori *et al.*, 2000).

Recent results indicate that one of the consequences of cholesterol effects on lipid traffic is the alteration of intracellular distribution of rab proteins. The cholesterol-accumulating drug U18666A increases the amounts of membrane-associated rab7 and inhibits rab7 membrane extraction by GDI (Lebrand *et al.*, 2002). The levels of rab4 were increased 1.5–2-fold in membrane fractions from Niemann-Pick fibroblasts, compared with normal human skin fibroblasts (Choudhury *et al.*, 2004). It is also shown that the capacity of rab5 and rab9 for GDI-mediated extraction from membranes is reduced in Niemann-Pick fibroblasts (Ganley and Pfeffer, 2006). The authors also demonstrated that cholesterol stabilizes rab proteins directly in liposome experiment.

It is intriguing that different rab proteins are affected by cholesterol-accumulating disease and cholesterol-accumulating reagent. Although Niemann-Pick mutations and U18666A accumulate cholesterol in late endosomes/lysosomes, U18666A causes pleiotropic effects on cellular cholesterol homeostasis (Liscum and Underwood, 1995). These results suggest that different rab proteins are affected by different modification of cellular cholesterol. These results also suggest that a new method of modifying cholesterol might uncover a new role of cholesterol in regulating rab proteins as well as lipid traffic. It is reported that cholesterol increase three to four times upon reaching confluence in cultured endothelial cells (Cansell *et al.*, 1997; Corvera *et al.*, 2000). In the present study, we found that the content and distribution of cellular cholesterol were altered when cells approach confluency in Chinese hamster ovary (CHO) cells. Comparison of subconfluent and confluent cells provides another system to examine the role of cholesterol on lipid traffic without using drugs or mutations involved in cholesterol homeostasis. We examined the internalization of several lipid probes in subconfluent and confluent CHO cells. Interestingly, the internalization of a subset of lipid probes was altered by cell confluency. This alteration was accompanied by redistribution of rab11. Cholesterol depletion from confluent cells diminished these alterations. These results suggest that cholesterol controls endocytic routes of a subset of lipid components through rab11.

MATERIALS AND METHODS

Chemicals and Antibodies

Poly(ethylene glycol)-derived cholesterol (PEG-cholesterol) was prepared as described (Sato *et al.*, 2004). Filipin was purchased from Polysciences (Warrington, PA). 22-(*N*-(7-nitrobenz-2-oxa-1,3-diazol-4-yl)amino)-23,24-bisnor-5-cholen-3β-ol (NBD-cholesterol), *N*-(4,4-difluoro-5,7-dimethyl-4-bora-3a,4a-diaza-s-indacene-3-pentanoyl)sphingosylphosphorylcholine (BODIPY-SM), *N*-((6-(7-nitrobenz-2-oxa-1,3-diazol-4-yl)amino)hexanoyl)sphingosylphosphorylcholine (NBD-SM), *N*-(4,4-difluoro-5,7-dimethyl-4-bora-3a,4a-diaza-s-indacene-3-pentanoyl)sphingosyl 1-β-D-lactoside (BODIPY-LacCer), Alexa Fluor 546–conjugated transferrin and Alexa Fluor-conjugated second antibodies were from Molecular Probes (Eugene, OR). Rabbit anti-γ-tubulin antibody and lipoprotein-deficient bovine serum (LPDS) were from Sigma (St. Louis, MO), goat anti-aldolase A polyclonal IgG was from Santa Cruz Biotechnology (Santa Cruz, CA). All other antibodies were form BD Transduction Laboratories (San Diego, CA). Methyl-β-cyclodextrin (MβCD) was from Cyclolab (Budapest, Hungary). [^{32}P]orthophosphate was from Perkin Elmer (Boston, MA). Phosphate-free Dulbecco's modified Eagle's medium (DMEM) and dialyzed fetal bovine serum were from GIBCO Invitrogen (Carlsbad, CA).

Plasmids

pDsRed-Monomer-Golgi (human galactosyltransferase) vector (DsRed-GalT) was purchased from BD Clontech (Palo Alto, CA). pEGFP-C1-rab4, -rab5, -rab7, and -rab11 were constructed as described previously (Fukuda, 2003; Tsuboi and Fukuda, 2006). A mutant rab11 containing an S25N or Q70L substitution was produced by conventional or two-step PCR techniques using the following mutagenic oligonucleotides with a restriction enzyme site (underlined) and substituted nucleotides (in boldface type) as described previously (Fukuda *et al.*, 1999): 5′-GGATCCATGGGCACCCGCGACGACGAGTACGACTACCTCTTTAAAGTTGTCCTTATTGGAGATTCTGGTGTTGGAAAGA**A**TAA-3′ (S25N primer, sense), 5′-CTC**GA**GCCCTGCTGTGTCCCATAT-3′ (Q70L primer 1, antisense), and 5′-C**TC**GAGCGGTACAGGGCTATAACG-3′ (Q70L primer 2, sense). The mutant rab11 fragments were subcloned into the BglII/EcoRI site of the pEGFP-C1 vector (BD Clontech) or the BamHI/NotI site of the pmRFP-C1 (BD Clontech) and verified by DNA sequencing as described previously (Tsuboi and Fukuda, 2005, 2006).

cDNA encoding mouse GDIα was amplified from Marathon-Ready adult mouse brain cDNA (BD Clontech) by PCR using the following pairs of oligonucleotides with a BamHI linker (underlined) or a stop codon (italics) as described previously (Fukuda *et al.*, 1999): 5′-GGATCCATGGATGAGGAATACGATGT-3′ (GDIα-Met primer; sense) and 5′-*TCA*CTGATCAGCTTCTCCAA-3′ (GDIα-stop primer; antisense). Purified PCR products were directly inserted into the pGEM-T Easy vector (Promega, Madison, WI) as described previously (Fukuda *et al.*, 1999). After verification by DNA sequencing, cDNA inserts were transferred to the pEF-T7 tag mammalian expression vectors (modified from pEF-BOS; Fukuda *et al.*, 1999), and the resultant plasmids are referred to as pEF-T7-GDIα.

Cell Culture

The CHO-K1 cell line was obtained from the American Type Culture Collection (ATCC; Manassas, VA). Cells were maintained in Ham's F-12 medium supplemented with 10% fetal calf serum (FCS), 100 U/ml penicillin, and 100 μg/ml streptomycin at 37°C.

Cellular Content of Cholesterol and Cholesteryl Ester

Cells, 1.9×10^5, were cultured in 140-mm dishes (to prepare subconfluent cell culture) and in 12-well plates (Φ23 mm, to obtain confluent cells) for 2 d. Cells, 1.28×10^6, were cultured in 60-mm dishes for 2 d to prepare cells treated with MβCD and LPDS.

Cells were then washed with phosphate-buffered saline (PBS) and scraped. A part of cell suspension was used for the determination of protein concentrations using a Bradford protein assay kit (Bio-Rad, Richmond, CA) or BCA protein assay kit (Pierce, Rockford, IL). Total lipids were extracted by the method of Bligh and Dyer (1959) and then separated by TLC with a solvent of hexane/diethyl ether/acetic acid (80:20:2, vol/vol). The lipids were visualized with phosphomolybdic acid (Nacalai Tesque, Kyoto, Japan), and cholesterol and cholesteryl ester were quantified by using a LAS1000plus luminescent imaging analyzer (Fuji Film, Tokyo, Japan).

Cell Staining

For filipin staining, 8.0×10^4 cells were cultured on coverslips in 90-mm dishes (subconfluent) and 24-well plates (Φ15 mm; confluent) for 2 d. The coverslips were rinsed in ice-cold PBS and fixed with 3% paraformaldehyde for 10 min at room temperature, followed by treatment with 50 mM NH_4Cl in PBS for 10 min and then were permeabilized with 50 μg/ml digitonin in PBS for 5 min. Cells were then doubly labeled with 50 μg/ml filipin and rabbit anti-γ-tubulin antibody in PBS followed by Alexa 546–conjugated anti-rabbit IgG. rab11 or rab4 staining was performed by the method of Chen *et al.* (1998) with a modification. Cells were washed with ice-cold PBS and permeabilized with 0.05% saponin (Sigma, St. Louis, MO) in 80 mM PIPES-KOH (pH 6.8), 5 mM EGTA, and 1 mM $MgCl_2$ for 5 min on ice and washed once with ice-cold PBS. Cells were fixed, followed by NH_4Cl treatment and then labeled with mouse anti-rab11 or -rab4 mAb overnight at 4°C. After the excess anti-rab11 and -rab4 antibodies were washed away, cells were incubated with Alexa 488–conjugated anti-mouse IgG. For double staining with anti-rab11 and -GM130 antibodies, cells were labeled with anti-rab11 antibody and Alexa Fluor-conjugated secondary antibody, followed by labeling with fluorescein isothiocyanate–conjugated anti-GM130 antibody.

Microscopy and Quantitation of Colocalization

The confocal images of cells doubly labeled with BODIPY-LacCer and DsRed-GalT were acquired on Fluoview FV1000 confocal microscope equipped with PLAPO 60XOLSM (1.1 NA) objective (Olympus, Tokyo, Japan). Other specimens were observed under LSM 510 confocal microscope equipped with C-Apochromat 63XW Korr (1.2 NA) objective (Carl Zeiss, Oberkochen, Germany). To quantitate colocalization, the Pearson correlation coefficient (r) was determined using LSM Image Examiner software version 3.2 (Carl Zeiss).

$$r = \frac{\sum_i (ch1_i - ch1_{aver}) \times (ch2_i - ch2_{aver})}{\sqrt{\sum_i (ch1_i - ch1_{aver})^2 \times \sum_i (ch2_i - ch2_{aver})^2}}$$

where *ch1i* and *ch2i* are the red and green intensities of voxel *i*, respectively, and *ch1aver* and *ch2aver* the average value of *ch1i* and *ch2i*, respectively. There is a positive correlation when *r* is higher than 0.2, whereas *r* between −0.2 and 0.2 indicates no correlation.

Incorporation of Fluorescent PEG-Cholesterol

Incorporation of fluorescent PEG-cholesterol was performed as described (Sato *et al.*, 2004) with a modification. Cells, 1.3×10^3, were grown in two-well chambers (4.2-cm^2 area; to obtain subconfluent cells; Lab-Tek Chambered Coverglass, Nalge Nunc International, Rochester, NY), or 8.6×10^3 cells were grown in eight-well chambers (0.8-cm^2 area; confluent cells) for 3 d. In Figure 7, 8.0×10^4 cells were grown in glass-bottom 24-well plates (Iwaki, Tokyo, Japan) for 2 d. Cells were incubated with 0.5 μM fluorescent PEG-cholesterol in DMEM/Nutrient mixture Ham's F-12, without phenol red (DMEM F-12, Sigma) for 1 min (subconfluent) or 5 min (confluent) at 15°C. Five minutes is required for confluent cells because of the low efficiency of insertion of PEG-cholesterol. After excess PEG-cholesterol was washed with DMEM F-12, cells were incubated for 15 min at 37°C. The specimens were treated with 10 mM NH_4Cl in DMEM F-12 medium before acquiring image. When doubly labeled with BODIPY-SM or Alexa 546–conjugated transferrin (Tf), cells were preincubated with 4 μM BODIPY-SM or 50 μg/ml Alexa-546 Tf in serum-free Ham's F-12 medium supplemented with 0.2% BSA for 30 min at 15°C. After washing, cells were labeled with PEG-cholesterol and incubated for a further 15 min at 37°C.

Incorporation of NBD-Cholesterol

Cells were incubated with 5 μg/ml NBD-cholesterol in 10% FCS containing Ham's F-12 medium. After 30 min at 10°C, cells were washed with DMEM F-12, followed by further incubation for 5 min at 37°C.

Incorporation of BODIPY-SM, NBD-SM, and BODIPY-LacCer

Cells were incubated with 4 μM BODIPY-SM or NBD-SM in 10% FCS containing Ham's F-12 medium. When cells were treated with MβCD or LPDS, BODIPY-SM was dispersed in 0.03 mg/ml fatty acid–free bovine serum albumin (BSA; Sigma) containing DMEM F-12. After 30 min at 10°C, cells were washed with DMEM F-12, followed by further incubation for 15 min at 37°C. Incorporation of BODIPY-LacCer was performed by the method of Sharma *et al.* (2004) with a modification. Cells were incubated with 2 μM BODIPY-LacCer in 10% FCS containing Ham's F-12 medium for 30 min at 10°C, washed with DMEM F-12, and further incubated for 15 min at 37°C, followed by back-exchange with 5% fatty acid free BSA.

Recycling Assay of NBD-SM

Cells, 8.0×10^4, were seeded in 90-mm dishes (subconfluent) and 24-well plates (confluent) and grown for 2 d. Internalization of NBD-SM at 37°C was performed by incubating cells with 4 μM NBD-SM for 30 min at 10°C, followed by washing with DMEM F-12 at 10°C and further incubation with prewarmed DMEM F-12 medium for 10 min at 37°C. For 16°C internalization, cells were labeled with NBD-SM for 60 min at 16°C and were washed with DMEM F-12 at 16°C. After internalization, cells were treated with 50 mM sodium dithionite (Nacalai Tesque) to quench the fluorescent lipids at the cell surface (Kobayashi *et al.*, 1992), followed by washing. Then 1 ml of 37°C chase medium (5% fatty acid free BSA in DMEM-F-12 medium) was added. This was defined as chase time 0. Cells were chased in the chase medium at 37°C for up to 60 min. At each time point, chase medium was collected, and prewarmed fresh chase medium was added to cells. At the end of a 60-min chase, cells were washed and scraped. The fluorescent lipids of chase medium and harvested cells were extracted by the method of Bligh and Dyer (1959). The fluorescent lipids were dissolved with ethanol, and fluorescence measurements were performed using a FP-6500 spectrofluorometer (Jasco, Tokyo, Japan).

Transfection

Cells grown to 90% confluence in 60- or 90-mm dishes were transiently transfected using Lipofectamine 2000 (Invitrogen) with 2 or 4 μg plasmid DNA, respectively. Transfection was carried out according to the manufacturer's instructions. After transfection, cells were incubated overnight at 37°C and then replated.

Analysis of GDP and GTP-bound to rab11

Cells, 2.0×10^5, transfected with EGFP-rab11 were seeded in 140-mm dishes or 12-well plates, and cells were grown for 2 d. Analysis of GDP and GTP-bound to rab11 was performed by the method of Satoh *et al.* (1988) with a modification. Cells were labeled for 3 h at 37°C with 0.33 mCi/ml [^{32}P]orthophosphate in phosphate-free DMEM supplemented with 10% dialyzed fetal bovine serum. The cells were washed, scraped, and lysed with immunoprecipitation buffer (50 mM Tris-HCl, pH 7.5, 20 mM $MgCl_2$, 150 mM NH_4Cl, 0.5% NP-40) containing protease inhibitor cocktail (Calbiochem, La-Jolla, CA). The cell lysate was immunoprecipitated using rabbit anti-GFP antibody (Molecular Probes) and protein G-Sepharose, and the immunoprecipitate was resolved by polyethyleneimine-cellulose TLC (Merck, Rahway, NJ) with a solvent of 1.0 M LiCl/1.8 M formic acid. Radiolabeled GDP and GTP were detected with BAS2000 Bio-imaging analyzer (Fuji Film). The molar ratio of rab-bound GTP was calculated as [GTP]/([GDP] × 1.5 + [GTP]) × 100.

Table 1. Cholesterol and cholesteryl ester content of subconfluent and confluent cells

	Cholesterol	Cholesteryl ester
Subconfluent	25.6 ± 1.8	3.5 ± 0.3
Confluent	46.5 ± 8.7	9.2 ± 1.1

Numbers are mean of triplicate experiments ± SE, expressed as nmol/mg protein.

MβCD and LPDS Treatment

Cells were rinsed in serum-free medium three times followed by the incubation with 10 mM MβCD in serum-free medium for 15 min at 37°C. For LPDS treatment, cells grown for 1 d were incubated with Ham's F-12 medium supplemented with 5% LPDS for 20 h at 37°C.

Subcellular Fractionation and Immunoblotting

Cells, 1.28×10^6, were seeded in 60-mm dishes and grown for 2 d. Cells were treated with MβCD or LPDS as described above. For fractionation of membrane and cytosol and for immunoblot, cells were washed three times with PBS, scraped in ice-cold homogenization buffer (10 mM HEPES, 250 mM sucrose containing protease inhibitor cocktail), and homogenized using a Handy microhomogenizer (NS-310E, MICROTEC Co., Chiba, Japan). Then fractionation and immunoblot were performed as described (Chen *et al.*, 1998).

RESULTS

Content and Distribution of Cholesterol Alter in a Cell Confluency–associated Manner in CHO Cells

We prepared subconfluent and confluent cultures of CHO cells by seeding the same number of cells to dishes of different sizes. As observed in endothelial cells (Cansell *et al.*, 1997; Corvera *et al.*, 2000), both cholesterol and cholesteryl ester increased as cells reached confluency (Table 1). The free cholesterol–specific antibiotic filipin (Sokol *et al.*, 1988; Sato *et al.*, 2004) weakly labeled the pericentriolar compartment, which colocalized with a centriole marker, γ-tubulin, in subconfluent cells (Figure 1). The pericentriolar staining pattern is reminiscent of the recycling endosome of CHO

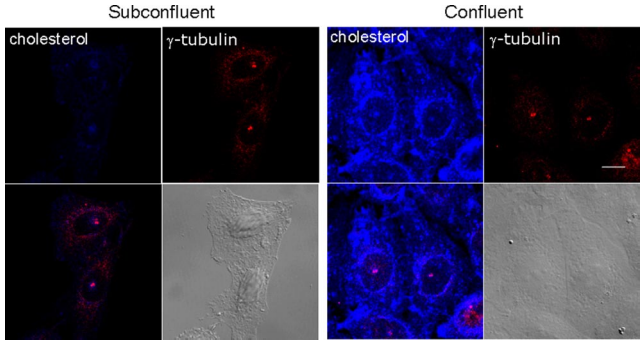

Figure 1. Cholesterol increases when CHO cells reach confluence. Subconfluent and confluent cells were doubly labeled with filipin and anti-γ-tubulin. Bar, 10 μm. Images were obtained under the same acquisition conditions (exposure time 1.97 s with laser power of 364 nm:5% and 543 nm:25%).

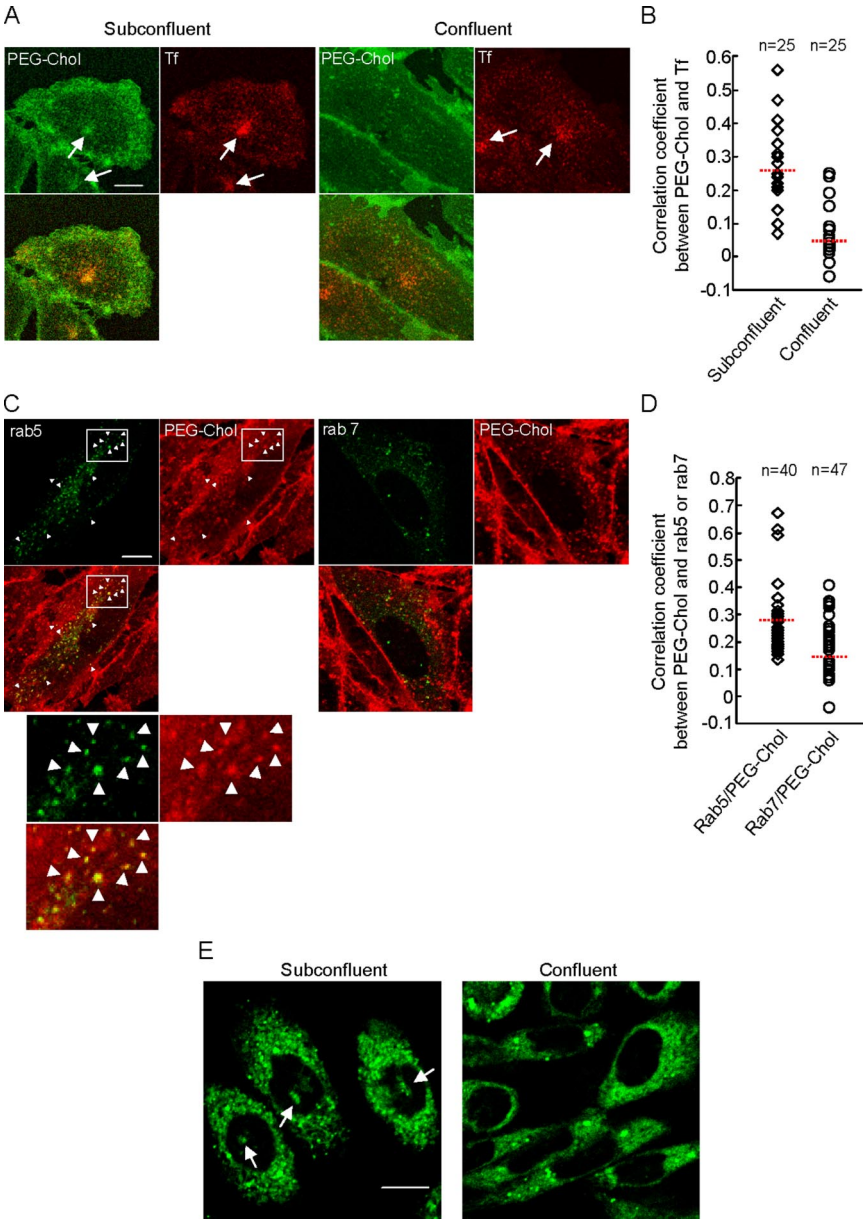

Figure 2. Cell confluency alters internalization of fluorescent PEG-cholesterol and NBD-cholesterol. (A) Subconfluent and confluent CHO cells transfected with human transferrin receptor were incubated with Alexa 546–conjugated transferrin (Tf) and fluorescein-PEG-cholesterol (PEG-Chol) for 15 min at 37°C. Arrows indicate pericentriolar recycling endosomes where incorporated transferrin was accumulated. Bar, 10 μm. (B) The correlation coefficients between the localization of internalized PEG-cholesterol and Alexa 546–conjugated Tf were calculated in subconfluent and confluent cells. ◇, subconfluent cells; ○, confluent cells. Dotted lines indicate the average values of subconfluent (0.262) and confluent cells (0.059). (C) Confluent CHO cells transfected with GFP-rab5 (rab5) or GFP-rab7 (rab7) were incubated with TRITC-PEG-cholesterol (PEG-Chol) for 15 min at 37°C. Arrowheads indicate colocalization of rab5 and TRITC-PEG-cholesterol. The enclosed areas are enlarged below. Bar, 10 μm. (D) The correlation coefficients between the localization of TRITC-PEG-cholesterol and GFP-rab5 or GFP-rab7 were calculated. ◇, rab5 and PEG-cholesterol; ○, rab7 and PEG-cholesterol. Dotted lines indicate the average values of rab5 and PEG-cholesterol (0.297), or rab7 and PEG-cholesterol (0.185). (E) Subconfluent and confluent CHO cells were incubated with NBD-cholesterol for 5 min at 37°C as described in *Materials and Methods.* Bar, 10 μm.

cells (Ullrich *et al.*, 1996). Filipin staining was much brighter in confluent cells. In confluent cells, in addition to pericentriolar fluorescence, the cell surface as well as perinuclear region, was intensely labeled with filipin.

Cell Confluency Alters Internalization of Fluorescent Lipid Probes

The above results indicate that the content and distribution of cellular cholesterol are significantly altered by cell confluency in CHO cells. In this study, we examined the internalization of several fluorescent lipid probes under these conditions (Figures 2 and 3). PEG derivative of cholesterol (PEG-cholesterol) preferentially partitions to specific membrane domains (Sato *et al.*, 2004). The bulk PEG moiety of PEG-cholesterol prevents transbilayer movement of the molecule. This inhibits the transport of PEG-cholesterol to the cytoplasmic leaflet and the nonspecific diffusion of the molecule to the cytoplasm when the molecule is inserted to the cell surface. Thus PEG-cholesterol could selectively monitor the endocytic pathway of plasma membrane subdomains. Subconfluent and confluent CHO cells were briefly labeled with the fluorescein ester of PEG-cholesterol (fluorescein-PEG-cholesterol), followed by washing excess compound and incubation at 37°C for 15 min. In subconfluent cells, internalized fluorescein-PEG-cholesterol was accumulated at the pericentriole region of cells, suggesting the transport of cell surface fluorescein-PEG-cholesterol to recycling endosomes. In contrast, in confluent cells, fluorescein-PEG-cholesterol was distributed in small vesicles throughout the cytoplasm. Although PEG-cholesterol selectively inhibits clathrin-independent endocytosis at high concentration, under our experimental conditions the presence of PEG-cholesterol did not inhibit internalization of fluorescent dextran, which is internalized via clathrin-independent mechanism (Sabharanjak *et al.*, 2002; Supplementary Figure 1). The recycling endosomes are characterized by the accumulation of transferrin internal-

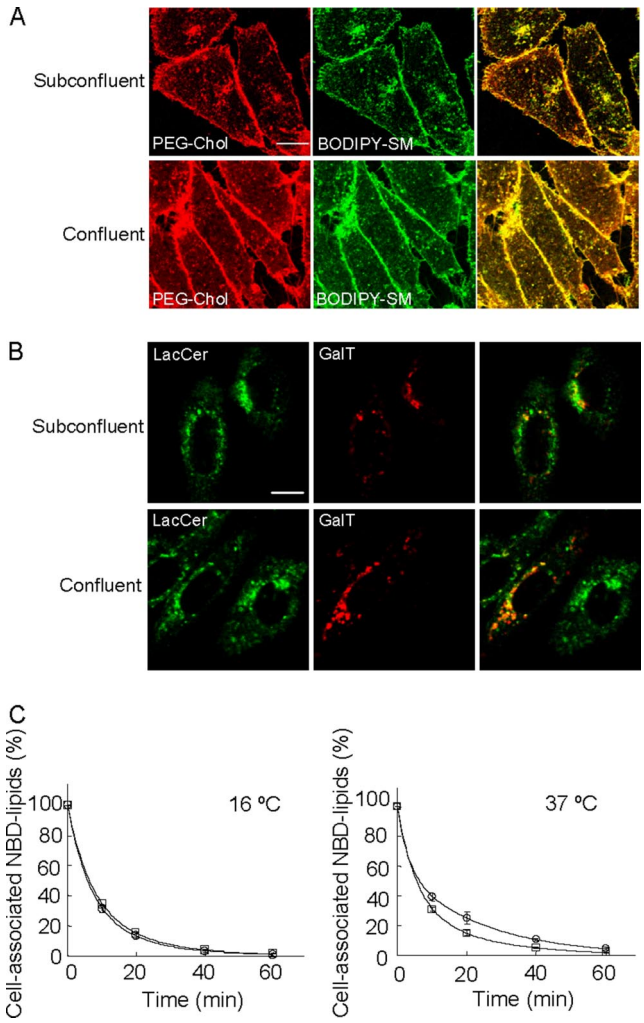

Figure 3. Cell confluency alters internalization and recycling of fluorescent SM but not the internalization of fluorescent LacCer. (A) Subconfluent and confluent cells were treated with TRITC-PEG-cholesterol (PEG-Chol) and BODIPY-SM for 15 min at 37°C. Bar, 10 μm. (B) Subconfluent and confluent cells transfected with DsRed-galactosyltransferase (GalT) were treated with BODIPY-LacCer (LacCer) for 15 min at 37°C. Bar, 10 μm. (C) Recycling of NBD-SM in subconfluent and confluent CHO cells. Recycling was measured as described in *Materials and Methods.* The percentage of cell-associated fluorescence was calculated for each time point. Double exponential decay fits are plotted. □, subconfluent cells; ○, confluent cells. Data points were derived from an average of triplicate experiments. Kinetic parameters from Figure 3 are listed in Table 2.

ization (Koval and Pagano, 1989; Mayor *et al.*, 1993). To confirm whether fluorescein-PEG-cholesterol was accumulated in recycling endosomes, we transfected human transferrin receptor to CHO cells, followed by doubly labeling cells with fluorescein-PEG-cholesterol and Alexa-546–labeled transferrin. Fluorescent transferrin was accumulated in the central region of the cells both in subconfluent and confluent culture. In subconfluent cells, internalized transferrin was colocalized with endocytosed fluorescein-PEG-cholesterol (Figure 2A). We calculated Pearson correlation coefficient to quantitate the colocalization between fluorescein-PEG-cholesterol and transferrin in subconfluent and confluent cells (Figure 2B). Clearly there is a higher correlation in subconfluent cells than in confluent cells, indicating that fluorescein-PEG-cholesterol is colocalized with transferrin in subconfluent cells, but not in confluent cells (Figure 2B). This result suggests that the endocytic route of fluorescein-PEG-cholesterol, but not of transferrin, alters in a cell confluency-associated manner.

rab5 and rab7 are known to localize in the early and late endosomes, respectively (Chavrier *et al.*, 1990; Soldati *et al.*, 1995). In Figure 2C, confluent cells transfected with green fluorescent protein (GFP)-labeled rab5 or rab7, were incubated with tetramethylrhodamine B isothiocyanate (TRITC)-labeled PEG-cholesterol. TRITC-PEG-cholesterol was internalized similarly to fluorescein-PEG-cholesterol (Sato and Kobayashi, unpublished results). The colocalization of GFP-rab5 and TRITC-PEG-cholesterol indicates that PEG-cholesterol is internalized into early endosomes in confluent cells (Figure 2C, arrowheads). In contrast to rab5, transfected rab7, a late endosome marker, was not significantly colocalized with internalized PEG-cholesterol (Figure 2C). Correlation coefficients between PEG-cholesterol and rab5 or rab7 show that positive correlation occurs only between rab5 and PEG-cholesterol (Figure 2D).

In Figure 2E, subconfluent and confluent CHO cells were labeled with 22-(*N*-(7-nitrobenz-2-oxa-1,3-diazol-4-yl)amino)-23,24-bisnor-5-cholen-3β-ol (NBD-cholesterol) at 10°C, followed by washing excess compound and incubation at 37°C for 5 min. It is suggested that NBD-cholesterol is internalized by fast lipid binding protein–mediated process and by slow endocytic pathway (Frolov *et al.*, 2000). When cells were incubated at low temperature, fluorescence was observed throughout cytoplasm in both subconfluent and confluent cells (not shown). After warming up, NBD-cholesterol was also accumulated at the pericentriole region in subconfluent cells. In contrast, pericentriole labeling was not observed in confluent cells. Quantitation indicates that 76.4% (185 of 242) of subconfluent cells internalized NBD-cholesterol in pericentriolar region, whereas this value is decreased to 28.0% (122 of 436 cells) in confluent cells.

In Figure 3A, we compared the internalization of BODIPY-SM with that of TRITC-PEG-cholesterol in subconfluent and confluent CHO cells. The colocalization of fluorescence indicates the internalization of both BODIPY-SM and PEG-cholesterol alters in a cell confluency-dependent manner. We also examined the internalization of BODIPY-LacCer in pDsRed-galactosyltransferase (DsRed-GalT) transfected CHO cells. GalT is localized in the Golgi apparatus (Sciaky *et al.*, 1997). BODIPY-LacCer was rapidly incorporated to the DsRed-GalT–positive region in both subconfluent and confluent cells (Figure 3B). These results indicate that cell confluency affects the internalization route of limited subset of molecules.

Fluorescent SM undergoes rapid recycling in CHO cells (Koval and Pagano, 1989; Mayor *et al.*, 1993; Hao and Maxfield, 2000). We compared the recycling kinetics of fluorescent SM in subconfluent and confluent cells. In this experiment, we used NBD-SM. NBD fluorescence is readily removed from the cell surface by serum albumin or water soluble quencher (Koval and Pagano, 1989; Kobayashi *et al.*, 1992). It is reported that the bulk of the molecules internalized at 37°C are recycled via the recycling endosomes, whereas those internalized at 16°C are recycled back to the plasma membrane from early endosomes without passing through the recycling endosomes (Ren *et al.*, 1998). In Figure 3C, NBD-SM was internalized either at 16 or 37°C, and the recycling of fluorescent lipid to the plasma membrane was monitored at 37°C. The fraction of lipid that was cell-associated at each chase time point was fit with a double exponential decay. Theoretical fits were then plotted as solid lines. As previously de-

Table 2. Kinetic parameters of the recycling of NBD-SM in subconfluent and confluent CHO cells

	a	b (min^{-1})	c	d (min^{-1})
16°C Pulse				
Subconfluent	0.59 ± 0.07	0.16 ± 0.01 (4.4)	0.41 ± 0.07	0.060 ± 0.005 (11.6)
Confluent	0.62 ± 0.07	0.17 ± 0.01 (4.2)	0.41 ± 0.07	0.063 ± 0.005 (11.0)
37°C Pulse				
Subconfluent	0.64 ± 0.02	0.19 ± 0.01 (3.7)	0.36 ± 0.02	0.048 ± 0.002 (14.2)
Confluent	0.41 ± 0.04	0.33 ± 0.13 (2.1)	0.59 ± 0.04	0.043 ± 0.002 (16.1)

Kinetic parameters were obtained by fitting data points to a double exponential decay equation: $I = ae^{-bt} + ce^{-dt}$. Numbers are mean of triplicate experiments ± SD. Half-time values (min) are provided in parentheses.

scribed (Hao and Maxfield, 2000), a double exponential decay accounts well for the data. When NBD-SM was internalized at 37°C, the decay curves were slightly but significantly different between subconfluent and confluent cells. Although the rapid recycling component accounted for 64% of the recycled population in subconfluent cells, this component decreased to 41% in confluent cells (Table 2). These results suggest that the confluency-dependent transport of NBD-SM to the different destinations results in the altered efficiency of lipid recycling. The decay curves were not significantly altered between subconfluent and confluent cells when the fluorescent lipid was internalized at 16°C (Figure 3C and Table 2).

Rab11 Changes Intracellular Distribution in Cell Confluency–dependent Manner

Rab proteins play crucial roles in intracellular membrane traffic (Zerial and McBride, 2001). Localization to distinct compartments is a prerequisite for rab proteins to catalyze proper vesicular transport. We investigated whether cell confluency affects the intracellular distribution of rab4 and rab11, which are involved in the recycling of internalized lipids and proteins (van der Sluijs *et al.*, 1992; Daro *et al.*, 1996; Choudhury *et al.*, 2004; Maxfield and McGraw, 2004). Cell confluency did not significantly alter intracellular distribution of rab4 (Figure 4A). In contrast, intracellular distribution of rab11 was dramatically changed when cells reached confluence. In subconfluent cells, endogenous rab11 was diffusely distributed throughout the cell with partial enrichment in the perinuclear region which is partially colocalize with the Golgi marker, GM130 (Figure 4, A and B). Transfected GFP-rab11 was similarly distributed, whereas the enrichment in the perinuclear region was more prominent. In marked contrast, both endogenous and GFP-rab11 are concentrated in the pericentriolar region and colocalize with γ-tubulin in confluent cells (Figure 4, A and B). Quantitation indicates that 13.5% (n = 163) of subconfluent cells show pericentriolar localization of endogenous rab11, whereas 74.3% (n = 261) of confluent cells accumulate rab11 in pericentriolar region.

Constitutive Active Form of rab11 Alters Internalization of Lipid Probes in Confluent Cells

Our results indicate simultaneous change of intracellular distribution of rab11 and the endocytosis of fluorescent lipid probes when cells approaching confluence. These results suggest that observed alteration of internalization of lipid probes is caused by the alteration of the rab11 activity. Previously it was shown that the transport of transferrin from the early endosomes to the recycling endosomes is slowed down by the overexpression of rab11S25N (dominant negative). In contrast, overexpression of rab11Q70L (constitutively active) induces marked accumulation of transferrin in the recycling compartment (Ullrich *et al.*, 1996; Ren *et al.*, 1998). Expression of GFP-rab11Q70L results in the accumulation of the protein in pericetriolar recycling endosomes as described previously (Ullrich *et al.*, 1996; Ren *et al.*, 1998). In GFP-rab11Q70L transfected cells, internalized TRITC-PEG-cholesterol was colocalized with GFP-rab11Q70L (Figure 5A, arrows). Among 14 transfected cells, GFP-rab11Q70L colocalized with internalized PEG-cholesterol in 13 cells. This is a marked contrast to the nontransfected cells in which TRITC-PEG-cholesterol was accumulated in small vesicles distributed in the cytoplasm (Figure 5A, small arrows). Incorporation of TRITC-PEG-cholesterol was not significantly affected by the expression of GFP-rab11S25N. Among 13 transfected cells, only one cell showed pericentriolar distribution of PEG-cholesterol. Similar to PEG-cholesterol, expression of RFP-rab11Q70L caused the accumulation of NBD-cholesterol to the pericentriolar compartment (Figure 5B, arrow). All 29 examined cells showed accumulation of NBD-cholesterol to the RFP-rab11Q70L–positive pericentriolar compartment. Intracellular distribution of NBD-cholesterol was not affected by expression of RFP-rab11S25N as observed in the incorporation of PEG-cholesterol. Twelve cells showed the accumulation of NBD-cholesterol in centriolar compartment in 60 transfected cells (20%). This is close to the value (28%) of nontransfected cells (Figure 2E). These results suggest that rab11 regulates the fate of the internalization of lipid probes and the activity of rab11 is modified when cells reach confluence.

Intracellular Distribution of rab11 and Internalization of Fluorescent Sphingomyelin Are Changed by Partial Depletion of Cholesterol from Confluent Cells

Accumulation of cholesterol in confluent cells suggests that cholesterol may play a role in the redistribution of rab11 and the alteration of the endocytic pathway of lipid probes. Cellular cholesterol content is modified by acute cholesterol depletion using MβCD (Rothblat *et al.*, 1999; Sato *et al.*, 2004) or by growing cells in LPDS. We then investigated the intracellular distribution of rab11 and the endocytic pathway of fluorescent SM after confluent cells were treated with MβCD and LPDS (Figure 6A). MβCD treatment resulted in redistribution of rab11 to diffuse localization in the cytoplasm and partial enrichment in the perinuclear region (top row, arrows). This was accompanied by the internalization of BODIPY-SM to the pericentriolar region of the cell (bottom row, arrows). This internalization is similar to that observed in subconfluent cells. Internalized BODIPY-SM was observed in pericentriolar region in 49.5% (44 of 200) of MβCD-treated cells. In contrast, 6.3% (10 of 158) of control

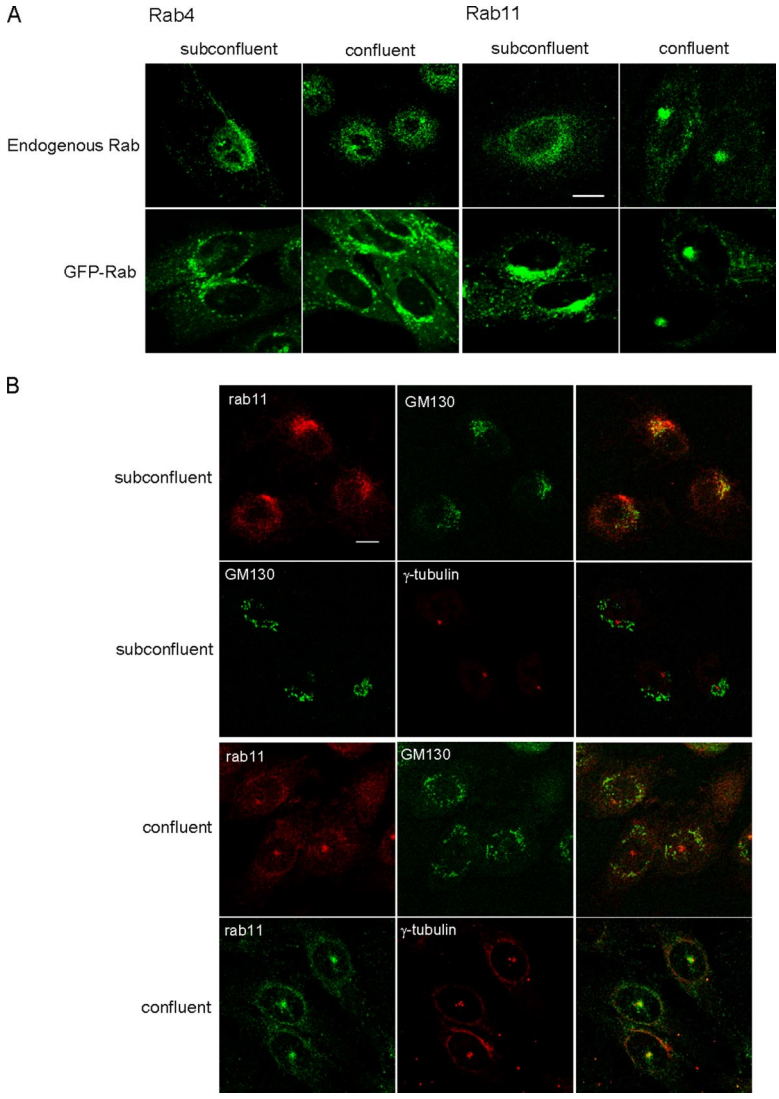

Figure 4. Cell confluency alters intracellular localization of rab11 but not rab4. (A) Localization of endogenous and GFP-rab4 and -rab11 in subconfluent and confluent CHO cells. Bar, 10 μm. (B) Subconfluent and confluent cells were labeled with anti-rab11, anti-GM130, and anti-γ-tubulin. Bar, 10 μm.

cells accumulated fluorescent SM in pericentriolar region. When cells were grown in LPDS medium, rab11 was diffusely distributed throughout cytoplasm. Under these conditions, fluorescent lipid was accumulated in the Golgi marker DsRed-GalT positive perinuclear region (Figure 6, A and B). The correlation coefficient (Figure 6B) shows positive correlation between internalized NBD-SM and DsRed-GalT. These results indicate that cellular level of cholesterol affects both intracellular distribution of rab11 and the internalization of fluorescent SM.

Rab proteins cycle between the membrane and cytosol. We then investigated whether cellular level of cholesterol affects the solubility of rab11. In Figure 6C, the distribution of rab11 in membrane and cytosol fractions was analyzed by Western blotting after MβCD or LPDS treatment. We verified that GS28 (Golgi SNARE), a membrane marker, and aldolase A, a cytosol marker, were concentrated in membrane and cytosol fractions, respectively (Figure 6C). The results were quantified and summarized in Table 3. Cholesterol contents after the treatments are also shown in Table 3. The soluble form of rab11 was increased from 48.8 $\pm$ 3.2% (mean of several experiments $\pm$ SE) to 54.2 $\pm$ 2.9 and 63.1 $\pm$ 1.2% by treating with MβCD and LPDS, respectively (Figure 6C, Table 3). This result suggests that cholesterol affects the membrane-cytosol cycle of rab11.

Cholesterol and Cell Confluency Do Not Affect GTP/GDP Ratio of rab11

Rab GTPases are in equilibrium between the inactive GDP-bound and activated GTP-bound states. GDI extracts only GDP-bound form of rab proteins and forms a complex with rab proteins in GDP-bound form in the cytosol (Alory, 2001; Pfeffer and Aivazian, 2004). It is possible that cholesterol increases the soluble form of rab11 by changing GTP/GDP ratio of rab11. We thus investigated whether GTP/GDP ratio of rab11 is changed in a cell confluency– or cholesterol-dependent manner (Table 3, Supplementary Figure 2). In subconfluent cells, GTP-rab11 comprised 55.0 $\pm$ 1.2% (mean of triplicate $\pm$ SE) and in confluent cells, this value was 57.6 $\pm$ 1.1%. Similarly, there was also no significant difference in GTP/GDP ratio of rab11 between control cells and MβCD treated confluent cells. These results suggest that difference of the distribution, rather than the GTP-bound form/GDP-bound form ratio of rab11, is the major consequence of the difference in cell confluency and MβCD-treated cells.

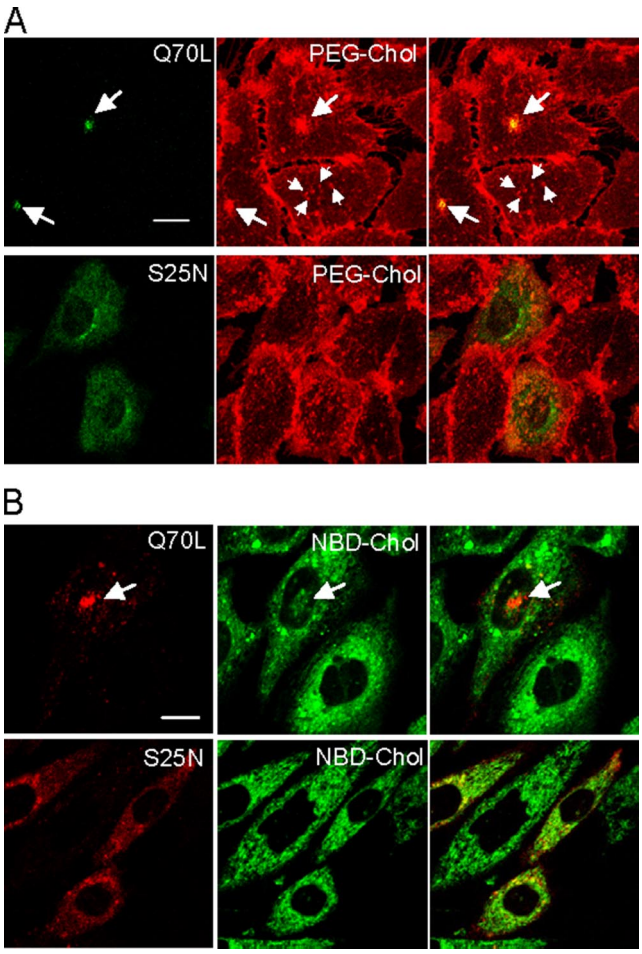

Figure 5. Constitutive active form of rab11 alters the endocytosis of PEG-cholesterol and NBD-cholesterol in confluent cells. (A) Confluent cells were transiently transfected with GFP-rab11Q70L (constitutive active) or GFP-rab11S25N (dominant negative). Cells were then incubated with TRITC-PEG-cholesterol for 15 min at 37°C. Arrows indicate pericentriolar recycling endosomes where GFP-rab11Q70L is accumulated, whereas small arrows indicate small vesicles in cytoplasm. Bar, 10 μm. (B) Confluent cells transfected with RFP-rab11Q70L or RFP-rab11S25N were incubated with NBD-cholesterol for 5 min at 37°C. Arrows indicate pericentriolar recycling endosomes where GFP-rab11Q70L is accumulated. Bar, 10 μm.

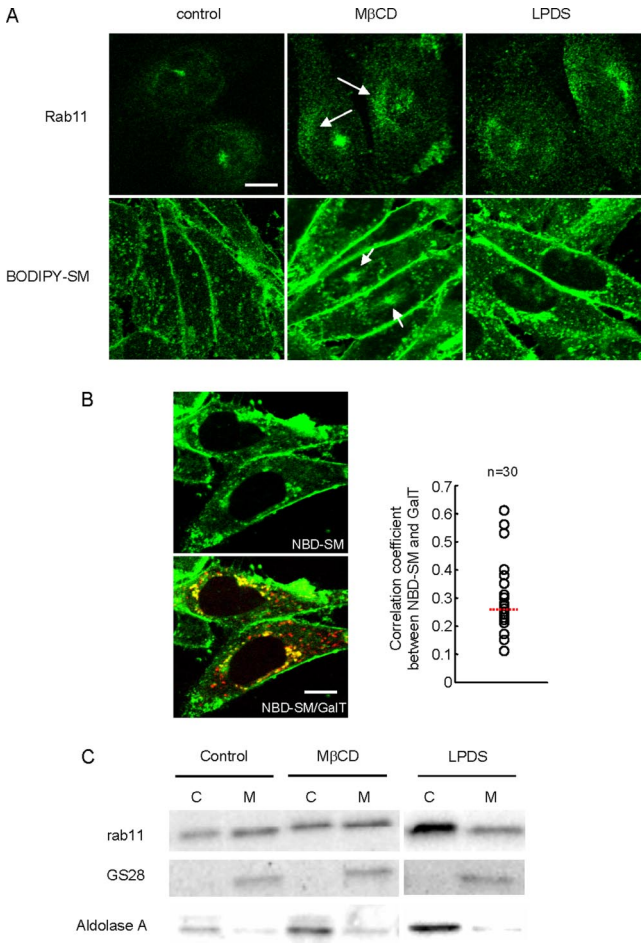

Figure 6. (A) MβCD and LPDS treatment alter rab11 distribution and the internalization of fluorescent SM in confluent cells. (A) Cells were treated with MβCD or LPDS as described in *Materials and Methods.* Cells were then fixed, labeled with anti-rab11 antibody, and processed for confocal microscopy. Internalization of BODIPY-SM was measured as described in *Materials and Methods.* Arrows indicate diffuse localization of rab11 in cytoplasm and pericentriolar accumulation of BODIPY-SM. Bar, 10 μm. (B) Cells transfected with DsRed-GalT were treated with LPDS. Then, the internalization of NBD-SM was measured as described in *Materials and Methods.* The correlation coefficients between the localization of NBD-SM and DsRed-GalT were calculated. Dotted line indicates the average value (0.270). Bar, 10 μm. (C) After MβCD or LPDS treatment, cells were homogenized and cytosol (C) and membrane (M) fractions were prepared as described in *Materials and Methods.* Fractions were analyzed by Western blotting with antibody against rab11. The amount of GS28 and aldolase A were analyzed as markers of membrane and cytosol, respectively. The data are calculated and displayed in Table 3.

Overexpression of GDI Redistributes rab11 and Fluorescent Lipid Probes in Confluent Cells

Our results suggest that intracellular distribution of rab11 determines the fate of fluorescent lipid probes. The present results also suggest that cholesterol controls the distribution of rab11. One possible explanation of our results is that the accumulation of cholesterol in confluent cells diminishes the extraction of rab11 by GDI, as observed in other rab proteins (Lebrand *et al.,* 2002; Choudhury *et al.,* 2004; Ganley and Pfeffer, 2006). Excess GDI added in vitro has been demonstrated to release GDP-bound rab proteins from membranes by forming a soluble complex (Dirac-Svejstrup *et al.,* 1994; Peter *et al.,* 1994; Ullrich *et al.,* 1994; Lebrand *et al.,* 2002; Choudhury *et al.,* 2004; Ganley and Pfeffer, 2006). Chen *et al.* (1998) demonstrated that rab11 is selectively released from membranes by the overexpression of GDI. In Figure 7, we overexpressed GDIα and examined the intracellular distribution of rab11 and the distribution of endocytosed fluorescein-PEG-cholesterol in confluent CHO cells. Overexpression of GDIα significantly altered the distribution of rab11. Fluorescence was observed throughout the cytoplasm with partial enrichment in the perinuclear region. Overexpression of GDIα slightly increased cytosolic rab11 (42.6 $\pm$ 1.9 to 48.0 $\pm$ 0.9%, n = 3). Internalized fluorescein PEG-cholesterol was observed in pericentriolar region in 5.9% (11 of 186) of nontransfected cells. This value was increased to 15.0% (32 of 213) by the transfection of GDIα. In addition to PEG-cholesterol, overexpression of GDIα (40.6%, n = 653) increased the number of cells with pericentriolar staining pattern of NBD-cholesterol compared with mock-transfected cells (23.4%, n = 788).

Table 3. Cellular cholesterol content and soluble and GTP-form of rab11 in different conditions

	Control	MβCD	LPDS
Cholesterol content (nmol/mg protein)	57.1 ± 5.3 (6)	50.5 ± 4.2 (5)	46.4 ± 4.0 (4)
% of soluble form rab11	48.8 ± 3.2 (8)	54.2 ± 2.9 (5)	63.1 ± 1.2 (4)
% of GTP-bound form rab11	59.5 ± 0.7 (3)	56.4 ± 2.1 (3)	Not determined

	Subconfluent	Confluent
% of GTP-bound form rab11	55.0 ± 1.2 (3)	57.6 ± 1.1 (3)

Numbers are mean ± SE of several experiments, with n values in parentheses.

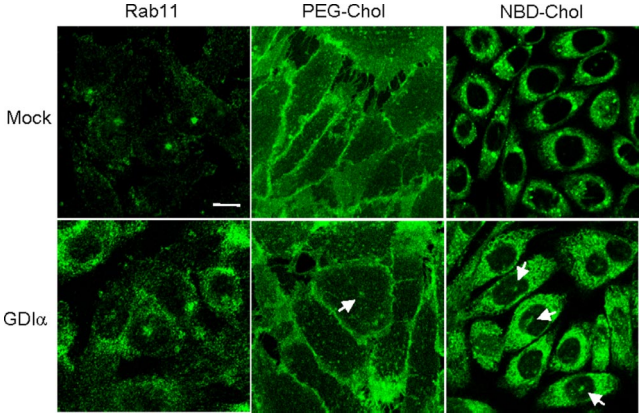

Figure 7. Overexpression of GDI redistributes rab11 and fluorescent cholesterol probes in confluent cells. Confluent CHO cells were transiently transfected with mock or GDIα. Cells were then fixed and labeled with anti-rab11. Internalization of fluorescent PEG-cholesterol or NBD-cholesterol was measured as described in *Materials and Methods.* Arrows indicate pericentriolar accumulation of fluorescence. Bar, 10 μm.

DISCUSSION

Present results indicate that both content and distribution of cholesterol alters in CHO cells when cells approach confluency. This is accompanied by the altered internalization of several lipid probes. Present study suggests that the internalization of fluorescent lipid probes is dependent on intracellular distribution of rab11, which is modified by changing cellular level of cholesterol.

Previously it was shown that NBD-SM is internalized into recycling endosomes together with transferrin in CHO cells (Koval and Pagano, 1989; Mayor *et al.*, 1993). Our results also indicate fluorescent SM analogs were internalized together with fluorescent PEG-cholesterol (Sato *et al.*, 2004) into pericentriolar recycling endosomes in subconfluent cells. In addition, NBD-cholesterol was accumulated into the pericentriolar compartments. However, in confluent cells, these fluorescent lipid probes did not reach the pericentriolar endosomes, whereas transferrin was transported to pericentriolar compartments. BODIPY-LacCer was transported to the Golgi apparatus both in subconfluent and confluent cells. These results indicate that cell confluency affects the endocytic pathways of limited number of plasma membrane components. It is reported that during endocytosis cargo moves through distinct domains on endosomes (Sonnichsen *et al.*, 2000). BODIPY-LacCer is internalized almost exclusively by a clathrin-independent mechanism, whereas BODIPY-SM is taken up approximately equally by clathrin-dependent and -independent pathways in human skin fibroblasts (Puri *et al.*, 2001). Transferrin is a well-known marker of clathrin-dependent endocytosis (Hanover *et al.*, 1984). The above observations suggest that these cargos are distributed in different membrane domains in early endosomes. The results thus suggest that the transport of specific lipid domains from early endosomes to recycling endosomes is delayed when cells reach confluence.

We demonstrated that the recycling rate of NBD-SM was delayed in confluent cells when the fluorescent lipid was internalized at 37°C. However, there was no significant difference of lipid recycling when NBD-SM was internalized at 16°C. It is reported that the bulk of the molecules internalized at 16°C are recycled back to the plasma membrane from early endosomes without passing through the recycling endosomes (Ren *et al.*, 1998). Our results thus suggest that cell confluency affects the transport of NBD-SM from early endosomes to the recycling endosomes but not from the early endosomes to the plasma membrane. Rab11 regulates recycling through the pericentriolar recycling endosomes (Ullrich *et al.*, 1996; Ren *et al.*, 1998), whereas rab4 is suggested to play a role in fast recycling from early endosomes back to the plasma membrane (van der Sluijs *et al.*, 1992; Sheff *et al.*, 1999). Our results suggest that rab11-mediated recycling is selectively modified during cell confluency. Consistent with this, our results indicated that intracellular distribution of rab11, but not rab4, altered in a cell confluency–dependent manner. In subconfluent cells, rab11 was dispersed throughout the cytoplasm in addition to some enrichment in the perinuclear region. In contrast, rab11 was concentrated in the pericentriolar recycling endosomes in confluent cells. It has been reported that the distribution of rab11 varies in different cell types (Ullrich *et al.*, 1996; Green *et al.*, 1997; Casanova *et al.*, 1999; Brown *et al.*, 2000; Sonnichsen *et al.*, 2000; van Ijzendoorn *et al.*, 2003). Our results suggest that this is in part because of the cell confluency-dependent redistribution of rab11.

When constitutive active rab11Q70L was expressed in confluent cells, the endocytosed fluorescent PEG-cholesterol and NBD-cholesterol were accumulated in the recycling endosomes. In contrast, dominant negative rab11S25N did not alter the internalization of these lipid probes. These results also support the idea that the endocytosis of examined lipid probes to the recycling endosomes is under the control of rab11. Holtta-Vuori *et al.* (2002) demonstrated that the transient overexpression of rab11 resulted in prominent accumulation of free cholesterol in rab11-positive organelles and inhibited cellular cholesterol esterification. It is suggested that in rab11-overexpressing cells, deposition of cholesterol in recycling endosomes results in its impaired esterification, presumably due to defective recycling of cholesterol to the

plasma membrane. Our results showed that PEG-cholesterol and slowly internalized NBD-cholesterol were accumulated where constitutive active rab11 was expressed. Previously we showed that in vitro PEG-cholesterol is preferentially partitions to cholesterol-rich membranes (Sato *et al.*, 2004). It is shown that NBD-cholesterol is internalized into both mitochondria, where endogenous cholesterol is not accumulated, and recycling endosomes. In recycling endosomes, NBD-fluorescence was colocalized with the fluorescence of internalized dehydroergosterol (DHE; Mukherjee *et al.*, 1998). Precise distribution of PEG-cholesterol and NBD-cholesterol on the plasma membrane is not known. However, our results, together with the results of Holtta-Vuori, suggest that PEG-cholesterol and slowly internalized NBD-cholesterol may represent, at least in part, the fate of cell surface cholesterol. It has been reported that the Golgi targeting of internalized BODIPY-LacCer is dependent on rab7 and rab9 but is independent of rab11 (Choudhury *et al.*, 2002). This is consistent with our results that BODIPY-LacCer was transported to the Golgi apparatus in both subconfluent and confluent cells.

Present results indicate that the partial depletion of cholesterol from confluent cells alters intracellular distribution of rab11, suggesting that cholesterol controls the distribution of rab11 in a cell confluency–associated manner. MβCD treatment did not alter GTP-bound form/GDP-bound form ratio of rab11. However, the significant increase in soluble form of rab11 was accompanied by cholesterol depletion by MβCD or LPDS in confluent cells in vivo. It has been reported that accumulation of cholesterol inhibits GDI-dependent extraction of rab proteins from the endosomes (Lebrand *et al.*, 2002; Choudhury *et al.*, 2004; Ganley and Pfeffer, 2006). When cells were treated with hydrophobic amine, U18666A, cholesterol is accumulated in late endosomes (Liscum and Faust, 1989; Kobayashi *et al.*, 1999). This increases the amounts of late endosome membrane-associated rab7 and inhibits the extraction of membrane-bound rab7 by GDI (Lebrand *et al.*, 2002). This results in the loss of bidirectional mobility of late endosomes. In vitro extraction of rab4, rab9, and rab5 with GDI is severely attenuated in endosomal fractions from human skin fibroblasts derived from Niemann-Pick patients (Choudhury *et al.*, 2004; Ganley and Pfeffer, 2006). In confluent CHO cells, cholesterol was accumulated in both pericentriolar compartments and the plasma membrane. This may lead to the attenuation of the extraction of rab11 from the pericentriolar recycling endosomes.

MβCD treatment not only altered the intracellular distribution of rab11 but changed the internalization of BODIPY-SM in confluent cells. After treating cells, BODIPY-SM was incorporated into pericentriolar organelle as observed in subconfluent cells. These results suggest that cholesterol controls cell confluency–dependent endocytic pathway of a subset of lipid probes via rab11. PEG-cholesterol and NBD-cholesterol were accumulated in the recycling endosomes in confluent cells by overexpression of GDI, suggesting that importance of cellular distribution of rab11 on the endocytic pathway of these lipid probes. Choudhury *et al.* (2004) reported that the extraction of rab11 by GDI was not affected by cholesterol depletion in Niemann-Pick A and C fibroblasts in vitro. The difference could be explained that in Niemann-Pick cells, cholesterol is mainly accumulated in early and late endosomes, whereas preferential accumulation of cholesterol in recycling endosomes may occur when cells approach confluence. Furthermore, these differences in cholesterol distribution could account for different rabs inhibition by high levels of cellular cholesterol between Niemann-Pick cells and confluent CHO cells.

In summary, present study suggests that cholesterol controls the endocytosis of a limited subset of lipid probes by modulating rab11 distribution in a cell confluency–dependent manner. This is caused by the inhibition of extraction of rab11 by GDI under high cellular cholesterol condition. The mechanism(s) for cholesterol-regulated inhibition of GDI extraction of rab proteins is not well understood. Whereas the involvement of specific membrane constituents are proposed (Choudhury *et al.*, 2004), recent results using cholesterol containing liposomes suggest that cholesterol alone can influence rab retrieval from membranes (Ganley and Pfeffer, 2006). Further studies are required to understand the molecular mechanisms of cholesterol-dependent regulation of rab proteins.

ACKNOWLEDGMENTS

We are grateful to T. Hayakawa for the kinetic analyses. We thank members of Kobayashi laboratory and A. Yamaji-Hasegawa for critical reading of the manuscript and technical advice. We also thank members of Nakano laboratory of RIKEN, especially A. Nakano and R. Hirata for their support. This work was supported by grants from the Ministry of Education, Science, Sports, and Culture of Japan (16044247 and 17390025), grants from RIKEN Frontier Research System, Bioarchitect Project of RIKEN, and International HDL Award Program to T.K.

REFERENCES

Alory, C., and Balch, W. E. (2001). Organization of the Rab-GDI/CHM superfamily: The functional basis for choroideremia disease. Traffic *2*, 532–543.

Bligh, E. G., and Dyer, W. J. (1959). A rapid method of total lipid extraction and purification. Can. J. Biochem. Physiol. *37*, 911–917.

Brown, P. S., Wang, E., Aroeti, B., Chapin, S. J., Mostov, K. E., and Dunn, K. W. (2000). Definition of distinct compartments in polarized Madin-Darby canine kidney (MDCK) cells for membrane-volume sorting, polarized sorting and apical recycling. Traffic *1*, 124–140.

Cansell, M., Gouygou, J. P., Jozefonvicz, J., and Letourneur, D. (1997). Lipid composition of cultured endothelial cells in relation to their growth. Lipids *32*, 39–44.

Casanova, J. E., Wang, X., Kumar, R., Bhartur, S. G., Navarre, J., Woodrum, J. E., Altschuler, Y., Ray, G. S., and Goldenring, J. R. (1999). Association of Rab25 and Rab11a with the apical recycling system of polarized Madin-Darby canine kidney cells. Mol. Biol. Cell *10*, 47–61.

Chavrier, P., Parton, R. G., Hauri, H. P., Simons, K., and Zerial, M. (1990). Localization of low molecular weight GTP binding proteins to exocytic and endocytic compartments. Cell *62*, 317–329.

Chen, W., Feng, Y., Chen, D., and Wandinger-Ness, A. (1998). Rab11 is required for trans-golgi network-to-plasma membrane transport and a preferential target for GDP dissociation inhibitor. Mol. Biol. Cell *9*, 3241–3257.

Choudhury, A., Dominguez, M., Puri, V., Sharma, D. K., Narita, K., Wheatley, C. L., Marks, D. L., and Pagano, R. E. (2002). Rab proteins mediate Golgi transport of caveola-internalized glycosphingolipids and correct lipid trafficking in Niemann-Pick C cells. J. Clin. Invest. *109*, 1541–1550.

Choudhury, A., Sharma, D. K., Marks, D. L., and Pagano, R. E. (2004). Elevated endosomal cholesterol levels in Niemann-Pick cells inhibit rab4 and perturb membrane recycling. Mol. Biol. Cell *15*, 4500–4511.

Corvera, S., DiBonaventura, C., and Shpetner, H. S. (2000). Cell confluence-dependent remodeling of endothelial membranes mediated by cholesterol. J. Biol. Chem. *275*, 31414–31421.

Daro, E., van der Sluijs, P., Galli, T., and Mellman, I. (1996). Rab4 and cellubrevin define different early endosome populations on the pathway of transferrin receptor recycling. Proc. Natl. Acad. Sci. USA *93*, 9559–9564.

Dirac-Svejstrup, A. B., Soldati, T., Shapiro, A. D., and Pfeffer, S. R. (1994). Rab-GDI presents functional Rab9 to the intracellular transport machinery and contributes selectivity to Rab9 membrane recruitment. J. Biol. Chem. *269*, 15427–15430.

Fukuda, M. (2003). Distinct Rab binding specificity of Rim1, Rim2, rabphilin, and Noc2. Identification of a critical determinant of Rab3A/Rab27A recognition by Rim2. J. Biol. Chem. *278*, 15373–15380.

Frolov, A., Perescu, A., Atshaves, B. P., So, P.T.C., Gratton, E., Serrero, G., and Schroeder, F. (2000). High density lipoprotein-mediated cholesterol uptake and targeting to lipid droplets in intact L-cell fibroblasts. A single and multiphoton fluorescence approach. J. Biol. Chem. *275*, 12769–12780.

Fukuda, M., Kanno, E., and Mikoshiba, K. (1999). Conserved N-terminal cysteine motif is essential for homo- and heterodimer formation of synaptotagmins III, V, VI, and X. J. Biol. Chem. *274*, 31421–31427.

Ganley, I. G., and Pfeffer, S. R. (2006). Cholesterol accumulation sequesters Rab9 and disrupts late endosome function in NPC1-deficient cells. J. Biol. Chem. *281*, 17890–17899.

Green, E. G., Ramm, E., Riley, N. M., Spiro, D. J., Goldenring, J. R., and Wessling-Resnick, M. (1997). Rab11 is associated with transferrin-containing recycling compartments in K562 cells. Biochem. Biophys. Res. Commun. *239*, 612–616.

Hanover, J. A., Willingham, M. C., and Pastan, I. (1984). Kinetics of transit of transferrin and epidermal growth factor through clathrin-coated membranes. Cell *39*, 283–293.

Hao, M., Lin, S. X., Karylowski, O. J., Wustner, D., McGraw, T. E., and Maxfield, F. R. (2002). Vesicular and non-vesicular sterol transport in living cells. The endocytic recycling compartment is a major sterol storage organelle. J. Biol. Chem. *277*, 609–617.

Hao, M., and Maxfield, F. R. (2000). Characterization of rapid membrane internalization and recycling. J. Biol. Chem. *275*, 15279–15286.

Hao, M., Mukherjee, S., Sun, Y., and Maxfield, F. R. (2004). Effects of cholesterol depletion and increased lipid unsaturation on the properties of endocytic membranes. J. Biol. Chem. *279*, 14171–14178.

Holtta-Vuori, M., Maatta, J., Ullrich, O., Kuismanen, E., and Ikonen, E. (2000). Mobilization of late-endosomal cholesterol is inhibited by Rab guanine nucleotide dissociation inhibitor. Curr. Biol. *10*, 95–98.

Holtta-Vuori, M., Tanhuanpaa, K., Mobius, W., Somerharju, P., and Ikonen, E. (2002). Modulation of cellular cholesterol transport and homeostasis by Rab11. Mol. Biol. Cell *13*, 3107–3122.

Kobayashi, T., Beuchat, M. H., Lindsay, M., Frias, S., Palmiter, R. D., Sakuraba, H., Parton, R. G., and Gruenberg, J. (1999). Late endosomal membranes rich in lysobisphosphatidic acid regulate cholesterol transport. Nat. Cell Biol. *1*, 113–118.

Kobayashi, T., Storrie, B., Simons, K., and Dotti, C. G. (1992). A functional barrier to movement of lipids in polarized neurons. Nature *359*, 647–650.

Kok, J. W., Babia, T., and Hoekstra, D. (1991). Sorting of sphingolipids in the endocytic pathway of HT29 cells. J. Cell Biol. *114*, 231–239.

Koval, M., and Pagano, R. E. (1989). Lipid recycling between the plasma membrane and intracellular compartments: transport and metabolism of fluorescent sphingomyelin analogues in cultured fibroblasts. J. Cell Biol. *108*, 2169–2181.

Lebrand, C., Corti, M., Goodson, H., Cosson, P., Cavalli, V., Mayran, N., Faure, J., and Gruenberg, J. (2002). Late endosome motility depends on lipids via the small GTPase Rab7. EMBO J. *21*, 1289–1300.

Linder, M. D., Uronen, R. L., Holtta-Vuori, M., van der Sluijs, P., Peranen, J., and Ikonen, E. (2007). Rab8-dependent recycling promotes endosomal cholesterol removal in normal and sphingolipidosis cells. Mol. Biol. Cell *18*, 47–56.

Liscum, L., and Faust, J. R. (1989). The intracellular transport of low density lipoprotein-derived cholesterol is inhibited in Chinese hamster ovary cells cultured with 3-beta-[2-(diethylamino)ethoxy]androst-5-en-17-one. J. Biol. Chem. *264*, 11796–11806.

Liscum, L., and Underwood, K. W. (1995). Intracellular cholesterol transport and compartmentation. J. Biol. Chem. *270*, 15443–15446.

Maxfield, F. R., and McGraw, T. E. (2004). Endocytic recycling. Nat. Rev. Mol. Cell Biol. *5*, 121–132.

Maxfield, F. R., and Wustner, D. (2002). Intracellular cholesterol transport. J. Clin. Invest. *110*, 891–898.

Mayor, S., Presley, J. F., and Maxfield, F. R. (1993). Sorting of membrane components from endosomes and subsequent recycling to the cell surface occurs by a bulk flow process. J. Cell Biol. *121*, 1257–1269.

Mukherjee, S., Soe, T. T., and Maxfield, F. R. (1999). Endocytic sorting of lipid analogues differing solely in the chemistry of their hydrophobic tails. J. Cell Biol. *144*, 1271–1284.

Mukherjee, S., Zha, X., Tabas, I., and Maxfield, F. R. (1998). Cholesterol distribution in living cells: fluorescence imaging using dehydroergosterol as a fluorescent cholesterol analog. Biophys. J. *75*, 1915–1925.

Narita, K., Choudhury, A., Dobrenis, K., Sharma, D. K., Holicky, E. L., Marks, D. L., Walkley, S. U., and Pagano, R. E. (2005). Protein transduction of Rab9 in Niemann-Pick C cells reduces cholesterol storage. FASEB J. *19*, 1558–1560.

Pagano, R. E. (2003). Endocytic trafficking of glycosphingolipids in sphingolipid storage diseases. Philos. Trans. R. Soc. Lond. B Biol. Sci. *358*, 885–891.

Peter, F., Nuoffer, C., Pind, S. N., and Balch, W. E. (1994). Guanine nucleotide dissociation inhibitor is essential for Rab1 function in budding from the endoplasmic reticulum and transport through the Golgi stack. J. Cell Biol. *126*, 1393–1406.

Pfeffer, S., and Aivazian, D. (2004). Targeting Rab GTPases to distinct membrane compartments. Nat. Rev. Mol. Cell Biol. *5*, 886–896.

Puri, V., Watanabe, R., Dominguez, M., Sun, X., Wheatley, C. L., Marks, D. L., and Pagano, R. E. (1999). Cholesterol modulates membrane traffic along the endocytic pathway in sphingolipid-storage diseases. Nat. Cell Biol. *1*, 386–388.

Puri, V., Watanabe, R., Singh, R. D., Dominguez, M., Brown, J. C., Wheatley, C. L., Marks, D. L., and Pagano, R. E. (2001). Clathrin-dependent and -independent internalization of plasma membrane sphingolipids initiates two Golgi targeting pathways. J. Cell Biol. *154*, 535–547.

Ren, M., Xu, G., Zeng, J., De Lemos-Chiarandini, C., Adesnik, M., and Sabatini, D. D. (1998). Hydrolysis of GTP on rab11 is required for the direct delivery of transferrin from the pericentriolar recycling compartment to the cell surface but not from sorting endosomes. Proc. Natl. Acad. Sci. USA *95*, 6187–6192.

Rothblat, G. H., de la Llera-Moya, M., Atger, V., Kellner-Weibel, G., Williams, D. L., and Phillips, M. C. (1999). Cell cholesterol efflux: integration of old and new observations provides new insights. J. Lipid. Res. *40*, 781–796.

Sabharanjak, S., Sharma, P., Parton, R. G., and Mayor, S. (2002). GPI-anchored proteins are delivered to recycling endosomes via a distinct cdc42-regulated, clathrin-independent pinocytic pathway. Dev. Cell *2*, 411–423.

Sato, S. B., Ishii, K., Makino, A., Iwabuchi, K., Yamaji-Hasegawa, A., Senoh, Y., Nagaoka, I., Sakuraba, H., and Kobayashi, T. (2004). Distribution and transport of cholesterol-rich membrane domains monitored by a membrane-impermeant fluorescent polyethylene glycol-derivatized cholesterol. J. Biol. Chem. *279*, 23790–23796.

Satoh, T., Endo, M., Nakamura, S., and Kaziro, Y. (1988). Analysis of guanine nucleotide bound to ras protein in PC12 cells. FEBS Lett. *236*, 185–189.

Sciaky, N., Presley, J., Smith, C., Zaal, K. J., Cole, N., Moreira, J. E., Terasaki, M., Siggia, E., and Lippincott-Schwartz, J. (1997). Golgi tubule traffic and the effects of brefeldin A visualized in living cells. J. Cell Biol. *139*, 1137–1155.

Sharma, D. K., Brown, J. C., Choudhury, A., Peterson, T. E., Holicky, E., Marks, D. L., Simari, R., Parton, R. G., and Pagano, R. E. (2004). Selective stimulation of caveolar endocytosis by glycosphingolipids and cholesterol. Mol. Biol. Cell *15*, 3114–3122.

Sheff, D. R., Daro, E. A., Hull, M., and Mellman, I. (1999). The receptor recycling pathway contains two distinct populations of early endosomes with different sorting functions. J. Cell Biol. *145*, 123–139.

Sokol, J. *et al.* (1988). Type C Niemann-Pick disease. Lysosomal accumulation and defective intracellular mobilization of low density lipoprotein cholesterol. J. Biol. Chem. *263*, 3411–3417.

Soldati, T., Rancano, C., Geissler, H., and Pfeffer, S. R. (1995). Rab7 and Rab9 are recruited onto late endosomes by biochemically distinguishable processes. J. Biol. Chem. *270*, 25541–25548.

Sonnichsen, B., De Renzis, S., Nielsen, E., Rietdorf, J., and Zerial, M. (2000). Distinct membrane domains on endosomes in the recycling pathway visualized by multicolor imaging of Rab4, Rab5, and Rab11. J. Cell Biol. *149*, 901–914.

Tsuboi, T., and Fukuda, M. (2005). The C2B domain of rabphilin directly interacts with SNAP-25 and regulates the docking step of dense core vesicle exocytosis in PC12 cells. J. Biol. Chem. *280*, 39253–39259.

Tsuboi, T., and Fukuda, M. (2006). Rab3A and Rab27A cooperatively regulate the docking step of dense-core vesicle exocytosis in PC12 cells. J. Cell Sci. *119*, 2196–2203.

Ullrich, O., Horiuchi, H., Bucci, C., and Zerial, M. (1994). Membrane association of Rab5 mediated by GDP-dissociation inhibitor and accompanied by GDP/GTP exchange. Nature *368*, 157–160.

Ullrich, O., Reinsch, S., Urbe, S., Zerial, M., and Parton, R. G. (1996). Rab11 regulates recycling through the pericentriolar recycling endosome. J. Cell Biol. *135*, 913–924.

van der Sluijs, P., Hull, M., Webster, P., Male, P., Goud, B., and Mellman, I. (1992). The small GTP-binding protein rab4 controls an early sorting event on the endocytic pathway. Cell *70*, 729–740.

van Ijzendoorn, S. C., Mostov, K. E., and Hoekstra, D. (2003). Role of rab proteins in epithelial membrane traffic. Int. Rev. Cytol. *232*, 59–88.

Walter, M., Davies, J. P., and Ioannou, Y. A. (2003). Telomerase immortalization upregulates Rab9 expression and restores LDL cholesterol egress from Niemann-Pick C1 late endosomes. J. Lipid Res. *44*, 243–253.

Zerial, M., and McBride, H. (2001). Rab proteins as membrane organizers. Nat. Rev. Mol. Cell Biol. *2*, 107–117.